Kinesin-1 Expressed in Insect Cells Improves Microtubule *in Vitro* Gliding Performance, Long-Term Stability and Guiding Efficiency in Nanostructures

Till Korten*, Samata Chaudhuri, Elena Tavkin, Marcus Braun, and Stefan Diez*

***Abstract*—The cytoskeletal motor protein kinesin-1 has been successfully used for many nanotechnological applications. Most commonly, these applications use a gliding assay geometry where substrate-attached motor proteins propel microtubules along the surface. So far, this assay has only been shown to run undisturbed for up to 8 h. Longer run times cause problems like microtubule shrinkage, microtubules getting stuck and slowing down. This is particularly problematic in nanofabricated structures where the total number of microtubules is limited and detachment at the structure walls causes additional microtubule loss. We found that many of the observed problems are caused by the bacterial expression system, which has so far been used for nanotechnological applications of kinesin-1. We strive to enable the use of this motor system for more challenging nanotechnological applications where long-term stability and/or reliable guiding in nanostructures is required. Therefore, we established the expression and purification of kinesin-1 in insect cells which results in improved purity and—more importantly—long-term stability >24 h and guiding efficiencies of >90% in lithographically defined nanostructures.**

***Index Terms*—Bionanotechnology, nanobioscience, nanostructures.**

I. Introduction

KINESIN-1 IS A cytoskeletal motor protein which moves along microtubules [1]. Because of its small size, energy efficiency, and relative stability in artificial environments, kinesin-1 has been intensively studied for nanotechnological applications [2], [3]. For example, kinesin-1 has been used for a smart-dust biosensor [4], for molecular cargo pick-up and drop-off [5], for the assembly of molecular cargo [6], for a blood type test [7], for the assembly of microtubule spools [8], and for the simultaneous detection of several proteins [9]. Typically these assays use the "gliding assay" geometry, where substrate-attached kinesin-1 motors propel microtubules along the surface. So far, long-term studies for microtubule gliding assays have shown that the assay can operate unperturbed (i.e., without replenishing microtubules) for several hours [10], [11]. After that time the main problem was that microtubules had disappeared, which is likely because of photodamage [10] in combination with molecular wear [12]. While a few hours are sufficient for the nanotechnological applications mentioned above, the run-time of the assay is currently preventing the use of molecular motors for more challenging applications such as parallel computation [13], [14] or high throughput screening. Low quality of motility is especially problematic for assays that use lithographically nanostructured surfaces that guide microtubules [15], [16]: Microtubules getting stuck in such structures are prone to block the transport paths, and cause following microtubules to detach. These problems have hampered the use of molecular motors in more intricate nanotechnological devices despite the fact that the tools are available and well understood for over a decade now [17]. Here, we demonstrate that part of the observed problems stem from the bacterial expression system which has so far been used for production of kinesin-1 motors for nanotechnological applications. Expression of eukaryote proteins in bacteria can cause problems because important chaperons are missing and premature translation termination leads to truncated proteins [18], [19]. To allow more challenging *in vitro* applications of motor proteins, we optimized the expression and purification of kinesin-1. We obtained highly pure and active kinesin-1 protein by expressing a histidine-tagged kinesin-1 construct from *drosophila melanogaster* in insect cells using a baculovirus vector. Exceptional purity was obtained using a two-step purification via an ion-exchange and a Ni-nitrilotriacetic acid (NTA) column. We compared this kinesin-1 (henceforth called "kinesin expressed in insect cells") to the same protein sequence expressed in *E. coli* (henceforth called "kinesin expressed in bacteria") and found greatly improved long-term stability >24

Manuscript received December 17, 2015; revised January 14, 2016; accepted January 14, 2016. Date of publication February 08, 2016; date of current version February 26, 2016. This work was supported by European Union Seventh Framework Programme (grant agreement number 613044, ABACUS), the European Research Council (Starting Grant No. 242933, NanoTrans), the European Social Funds (Grant No. 100111059, MindNano and Grant No. 100107464, ChemIT), and the German Research Foundation (Cluster of Excellence Center for Advancing Electronics Dresden and the Heisenberg Program). *Asterisks indicate corresponding authors.*

*T. Korten is with B CUBE—Center for Molecular Bioengineering and CFAED—Center for Advancing Electronics Dresden, Technische Universität Dresden, Dresden, Germany and with the Max Planck Institute of Molecular Cell Biology and Genetics, Dresden, Germany.

S. Chaudhuri, E. Tavkin, and M. Braun are with B CUBE—Center for Molecular Bioengineering and CFAED—Center for Advancing Electronics Dresden, Technische Universität Dresden, Dresden, Germany and with the Max Planck Institute of Molecular Cell Biology and Genetics, Dresden, Germany.

*S. Diez is with B CUBE—Center for Molecular Bioengineering and CFAED—Center for Advancing Electronics Dresden, Technische Universität Dresden, Dresden, Germany and with the Max Planck Institute of Molecular Cell Biology and Genetics, Dresden, Germany.

Color versions of one or more of the figures in this paper are available online at http://ieeexplore.ieee.org.

Digital Object Identifier 10.1109/TNB.2016.2520832

h and guiding efficiencies of >90% in lithographically defined nanostructures.

II. Methods

Unless noted otherwise, all chemicals were obtained from Sigma-Aldrich, Germany. All concentrations given are final concentrations.

A. Protein Expression and Purification

1) Purification of Tubulin: Porcine tubulin was purified from *porcine* brain (Vorwerk Podemus, Dresden, Germany) using established protocols as described previously [20].

2) Expression of Kinesin-1: Both kinesin-1 motor proteins used in this publication are based on the same protein sequence: A wild type kinesin-1 construct consisting of full length *drosophila melanogaster* kinesin-1 heavy chain (Dm KHC) [21] and a C-terminal histidine-tag. This protein was expressed either in bacteria as described in [21] or in SF9 insect cells using a baculovirus vector [22]. Expression in insect cells is ideal for *drosophila* kinesin-1 because these cells provide an environment (particularly chaperons and post-translational machinery) very similar to the one in which the motor protein is expressed *in vivo*. Insect cells were harvested by centrifugation at 200 $\times$ g for 15 min in a Heraeus Multifuge 3 S-R (Thermo Fisher Scientific). The pellet was resuspended in 10 ml phosphate buffered saline (total volume 20 ml) and snap frozen by slowly dropping individual droplets into liquid nitrogen.

3) Purification of Kinesin-1: Kinesin expressed in bacteria was purified as previously described [21]. The purification of kinesin expressed in insect cells was performed in two steps. First, the raw lysate was cleaned up on a cation exchange column. The flow-through from that column was slightly diluted and loaded onto a Ni-NTA column for affinity purification via the C-terminal histidine tag. The following two base buffers were used for the respective columns:

a) Cation buffer: 6.7 mM sodium acetate, 6.7 mM 4-(2-hydroxyethyl)-1-piperazineethanesulfonic acid (HEPES), 6.7 mM 2-ethanesulfonic acid (MES), pH 7.0, 20 mM beta mercaptoethanol (BME), 0.2 mM ATP, 0.2% (w/v) polyoxyethylene (20) sorbitan monolaurate (TWEEN20), 1x protease inhibitor cocktail (complete, EDTA free, Roche, Mannheim, Germany).

b) Nickel buffer: 50 mM sodium phosphate buffer, pH 7.5, 5% w/v glycerol, 300 mM KCl, 1 mM $MgCl_2$, 0.2% w/v TWEEN20, 10 mM BME, 0.1 mM ATP, 1x protease inhibitor cocktail.

Procedure for cation exchange column: 0.5 g cell pellet was lysed in 1.5 ml lysis buffer (cation buffer supplemented with TWEEN20 to a final concentration of 0.5% (w/v) and benzonase nuclease to a final concentration of 25 Units/mL) and centrifuged at 50000 rpm (MLA130 rotor, Beckman Optima 200 ultracentrifuge) for 30 min at 4°C, the supernatant (lysate) was loaded onto a cation exchange column (HiTrapSP(tm), 17-1151-01, GE Healthcare), washed with washing buffer (cation buffer supplemented with KCl to a final concentration of 50 mM) and eluted with elution buffer (cation buffer supplemented with KCl to a final concentration of 300 mM).

Procedure for Ni-NTA column: The eluate from the cation exchange column was diluted 5x in nickel loading buffer (nickel buffer supplemented with imidazole to a final concentration of 36 mM) and loaded onto a Ni-NTA column (HisTrap HP(tm), 17-5247-01, GE Healthcare), washed with nickel washing buffer (nickel buffer supplemented with KCl to a final concentration of 1000 mM and imidazole to a final concentration of 30 mM) and eluted with nickel elution buffer (nickel buffer supplemented with imidazole to a final concentration of 300 mM).

B. Microtubule Polymerization

1) Double-Stabilized Microtubules for Gliding Assays on Glass Surfaces: Because of their greater long-term stability, microtubules stabilized with both guanosine-5'-[(α,β)-methyleno]triphosphate (GMPCPP; Jena Bioscience, Germany) and taxol were used for long term gliding motility experiments on glass surfaces. Microtubules were polymerized from 0.2 mg/ml rhodamine labeled tubulin in BRB80 buffer (80 mM piperazine-N,N'-bis(2-ethanesulfonic acid) (PIPES)/KOH, pH 6.8, 1 mM ethylene glycol tetraacetic acid (EGTA), 1 mM $MgCl_2$) supplemented with $MgCl_2$ to a final concentration of 2 mM and GMPCPP to a final concentration of 1 mM. The polymerization mix was incubated on ice for 5 min and then for 2 h at 37°C. Afterwards, microtubules were centrifuged using a Beckman airfuge (Beckman, Brea, CA) at 100 000 xg for 5 min. The pellet was resuspended in a volume of 200 μl BRB80 containing 10 μM taxol. These microtubules were stable for up to 4 months at room temperature.

2) Taxol Stabilized Microtubules for Gliding Assays in Nanostructures: Because of their greater flexibility, microtubules stabilized only with taxol were used for gliding assays in nanostructures. Microtubules were polymerized from 4 mg/ml rhodamine labeled tubulin in BRB80 supplemented with $MgCl_2$ to a final concentration of 5 mM, Mg-GTP to a final concentration of 1 mM and DMSO to a final concentration of 5% (v/v) at 37 °C for 60 min. Afterwards, microtubules were stabilized and diluted 40-fold in BRB80 containing 10 μM taxol at room temperature.

C. Microtubule Gliding Assay

Microtubule gliding assays were performed as previously described [23]. Briefly, flow cells were constructed from two clean glass cover-slips (Menzel, 18 mm $\times$ 18 mm and 22 mm $\times$ 22 mm) or a glass coverslip and a structured Si chip, and separated by strips of Nescofilm (Roth). Flow cells were perfused with 15 μl casein-containing solution (0.5 mg/ml in BRB80) and left to adsorb for 5 min. Next, 15 μl of kinesin-1 solution (12.4 nM full-length kinesin-1 dimer for Figs. 2 and 3 and 25 nM for Fig. 4), was perfused into the flow cells and incubated for another 5 min. Thereafter, motility solution (1 mM ATP, 20 mM D-glucose, 20 μg/ml glucose oxidase, 10 μg/ml catalase, 10 mM DTT, 10 μM taxol in BRB80) containing rhodamine-labeled microtubules was applied. After 5 min, unbound microtubules were washed out with motility solution without microtubules.

For the long-term microtubule gliding assays, the channels were sealed using vacuum grease to prevent evaporation (which also prevented subsequent exchange of solutions). These assays were performed after the temperature of the microscope stage

had equilibrated to $25.26 \pm 0.06\,^{\circ}\mathrm{C}$ (mean $\pm$ standard deviation) throughout the duration of the experiment.

D. Preparation of Nanostructured Surfaces

The structures were similar to structures previously described in [15]. They consisted of an Au floor coated with kinesin-1 and 500 nm high SiO_2 walls and pedestals that were coated with poly(ethyleneoxy)-silane (PEG-silane) to prevent binding of motor proteins. Briefly, a 105 mm Si wafer was sputter-deposited with 100 nm-thick Au, sandwiched between two 10 nm-thick Ti adhesion layers. Next, a 500 nm-thick quartz layer was deposited, followed by a resist layer. After exposure in an optical lithography system, the resist was developed and the quartz layer was dry-etched down to the Au layer. Afterwards, chips were cleaned for 10 min in acetone and rinsed with ethanol and nanopure water. The SiO_2 was PEGylated for 16 h using 2.4 mg/ml 2-[Methoxy(polyethyleneoxy)propyl]trimethoxysilane, (PEG-silane; 90%; ABCR, SIM4492.7) in $\mathrm{Toluene} \cdot \mathrm{HCl}$. Finally, chips were rinsed in Toluene, Ethanol and nanopure water. All experiments were performed on chips that were processed identically and cut from the same wafer.

E. Imaging and Data Analysis

1) Imaging of Gliding Assays on Glass Surfaces: Fluorescence imaging was performed on a Nikon Eclipse Ti microscope equipped with a Perfect Focus System (PFS) using a 1.49 PlanApo 100x oil immersion objective. Rhodamine labeled microtubules were observed by epi-fluoroscence, excited with a metal arc lamp (Intensilight, Nikon), and a filter set for rhodamine (exec: 555/25. Dichroic LP 561, em: 609/54). Time-lapse images were recorded for 12 frames at a rate of 1 frame per second with an exposure time of 100 ms using an electron multiplying charge-coupled device (EMCCD) camera (iXon ultra EMCCD, DU-897U, Andor) in conjunction with NIS-Elements (Nikon) imaging software.

2) Imaging of Gliding Assays in Nanostructures: Fluorescence images were acquired using a Zeiss Axiovert 200M inverted optical microscope: Rhodamine labeled microtubules were observed by epi-fluorescence using a 40x air objective (Plan-Apochromat NA 0,95, Zeiss). Time-lapse images were recorded at a rate of 1 frame per second with an exposure time of 100 ms using an EMCCD camera (iXon+EMCCD, DU-897E, Andor) in conjunction with Metamorph imaging software (Universal Imaging Corp.)

Microtubule gliding velocities were evaluated using an automated MATLAB script based on a tracking algorithm developed in-house [24]. Guiding efficiencies were determined by hand by measuring the angle at which microtubules approached the wall, and then calculating the guiding efficiency as follows:

$$E = \frac{N_{guided}}{N_{tot}} \tag{1}$$

where E is the guiding efficiency, N_{guided} is the number of microtubules that were guided at the wall and N_{tot} is the total number of microtubules (guided microtubules and microtubules leaving the structure at the wall). The data was binned in 15° intervals. The error for the guiding efficiency (S_E) was estimated using the standard error of the mean of a binomial distribution:

$$S_E = \sqrt{\frac{E(1-E)}{N_{tot}}} \tag{2}$$

3) Quantification of Protein From Polyacrylamide Gel Electrophoresis (PAGE): Because of the impurity of the bacterial expression, the amount of full length kinesin-1 had to be measured by PAGE. First, the concentration of the pure kinesin expressed in insect cells was determined by advanced protein assay reagent (Cytoskeleton Inc., Denver, CO, USA). Then both the kinesin expressed in bacteria and the kinesin expressed in insect cells were run on the same gel. The intensity of the respective band corresponding to full-length kinesin-1 was measured using the gel analyzer tool from ImageJ (v.1.50b, National Institutes of Health, Bethesda, MD, USA). Finally, the amount of full-length kinesin expressed in bacteria was calculated from the measured amount of kinesin expressed in insect cells and the kinesin expressed in insect cells was diluted to match the concentration of full-length kinesin expressed in bacteria.

III. Results and Discussion

A. Microtubules Propelled by Kinesin Expressed in Insect Cells Stop Less

Direct comparison of kinesin expressed in bacteria and kinesin expressed in insect cells by PAGE (Fig. 1(a)) showed many impurities in the kinesin expressed in bacteria which have also been reported by others using the same expression and purification method (e.g., the band corresponding to full length kinesin-1 was reported to comprise 36% of the total protein in the supplementary methods of [25]). In contrast, only a single band was visible for kinesin expressed in insect cells. Encouraged by this result, we compared the performance of both kinesin-1 preparations in a gliding motility assay (see Fig. 1(b) for a schematic representation). In order to reduce molecular wear [12] and thus improve long-term stability, we used microtubules that were stabilized both with GMPCPP and taxol. We imaged these microtubules for the first time after 10 min (Fig. 2(a), (b)) and evaluated their frame-to-frame velocities using an automated MATLAB script (Fig. 2(c), (d)). The median (and 25–75 percentile) velocity of kinesin expressed in bacteria (755 (461–825) nm/s) was similar to velocities reported for double-stabilized microtubules published elsewhere [26], while microtubules propelled by kinesin expressed in insect cells were significantly faster (844 (771–898) nm/s, $p \ll 0.001$; Wilcoxon rank sum test). We noticed that some microtubules tended to stop intermittently. Therefore, the velocity distributions showed two peaks: one at nearly zero velocity (3 ± 19 nm/s and 1 ± 18 nm/s for kinesin expressed in bacteria and kinesin expressed in insect cells, respectively) and one around the full velocity of the motors (799 ± 74 nm/s and 854 ± 77 nm/s, respectively). The relative size of the peaks at zero velocity was much larger for kinesin expressed in bacteria than for kinesin expressed in insect cells. This discrepancy became even more pronounced after 3 h: For kinesin expressed in bacteria (Fig. 2(e), (g)) the stopping became much more severe and the peak at 2 ± 20 nm/s now

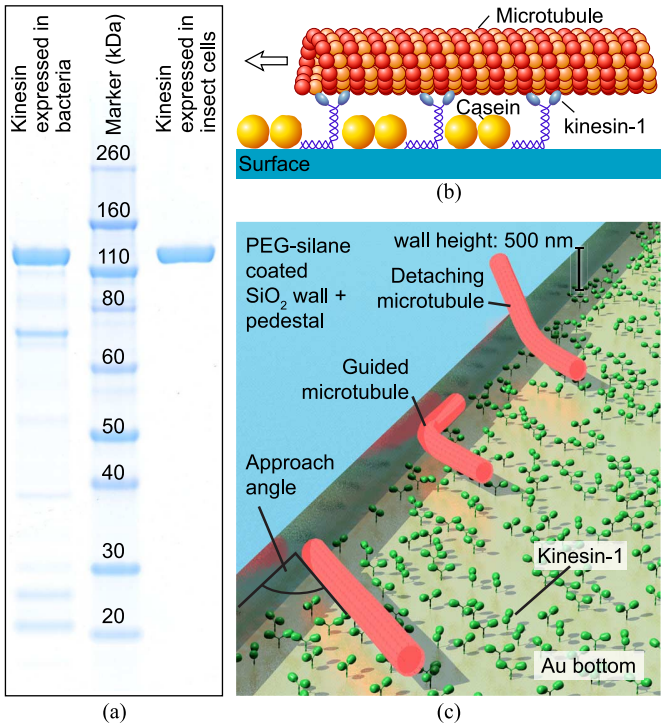

Fig. 1. Kinesin-1 purity and schematic representations of the motility assays. (a) PAGE of and kinesin expressed in bacteria compared to kinesin expressed in insect cells. (b) Schematic representation of a microtubule gliding assay. (c) 3D rendering of gliding microtubules being guided at a PEG-silane coated SiO_2 wall.

contained the majority of the frame-to-frame velocities while only a small fraction of microtubules was still moving (879 ± 57 nm/s). In contrast, the velocity distribution of microtubules propelled by kinesin expressed in insect cells (Fig. 2(f), (h)) showed only a negligible peak at 108 ± 75 nm/s and nearly all microtubules were moving with the full velocity of 900 ± 57 nm/s. During the first 3 h, the mean velocity of the fast populations of both motor protein expressions increased slightly by 80 nm/s and 46 nm/s for kinesin expressed in bacteria and insect cells, respectively. Because of the exponential dependence of microtubule gliding velocity on temperature [27], even a slight increase in temperature could explain an increased microtubule gliding velocity. While we did not measure an increase of the temperature at the microscope stage, we cannot exclude that the objective and sample itself heated up slightly because of light-absorption during imaging.

B. Microtubules Propelled by Kinesin Expressed in Insect Cells Move for More Than 24 h

Because we did not see a decline in gliding quality for kinesin expressed in insect cells within 3 h, we extended the assay time up to 26 h. Fig. 3(a) shows box plots of the velocity distributions of microtubules gliding on kinesin expressed in insect cells (light green) and kinesin expressed in bacteria (light blue). Apart from a slight initial increase in velocity, the median velocities for kinesin expressed in insect cells stayed the same over the entire experiment time. In contrast, the median velocities for kinesin expressed in bacteria were constant only for the first 40 min and then dropped rapidly and after 2 h, the majority of microtubules had stopped.

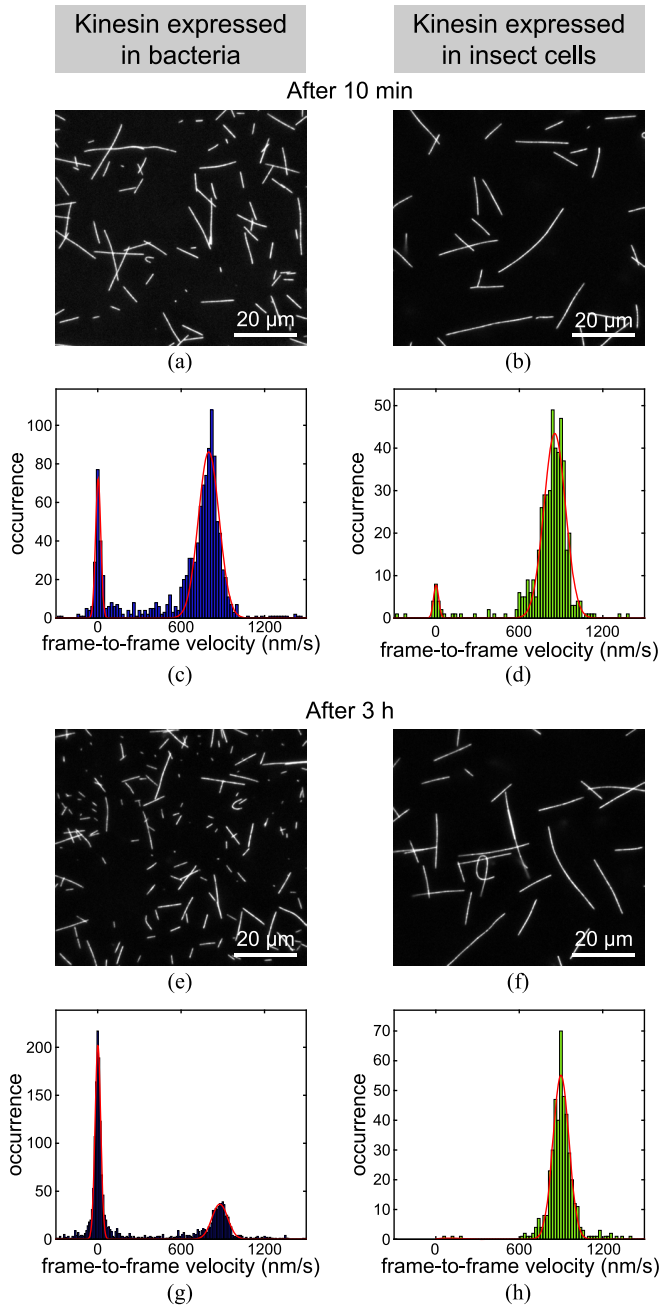

Fig. 2. Comparison of microtubule gliding assay performance using kinesin expressed in bacteria [(a), (c), (e), (g): blue bars] and kinesin expressed in insect cells [(b), (d), (f), (g): green bars]. Fluorescence micrographs [(a), (b), (e), (f)] and velocity distributions [(c), (d), (g), (h)] of kinesin gliding assays after 10 min [(a)–(d)] and after 3 h [(e)–(h)]. The velocity distributions represent the frame-to-frame velocities of 74 (c), 30 (d), 120 (c), and 28 (h) microtubules. The median (and 25^{th}–75^{th} percentiles) of the velocity distributions were: 755 (461–825) nm/s (c); 844 (771–898) nm/s (d); 21 (−6–806) nm/s (g); 902 (857–943) nm/s (h). The distributions were fitted with a double gaussian fit [red lines in (c), (d), (g), (h)] The results of the fits were (mean ± standard deviation of the fast and slow populations, respectively): 799 ± 74 nm/s and 3 ± 19 nm/s (c); 854 ± 77 nm/s and 1 ± 18 nm/s (d); 879 ± 57 nm/s and 2 ± 20 nm/s (g); 900 ± 57 nm/s and 108 ± 75 nm/s (h).

The observed stopping of microtubules was likely caused by non-motile motor proteins engaging in a tug-of-war with motile motors [28]. The stopping was much more pronounced for kinesin expressed in bacteria than for kinesin expressed in insect cells. We attribute the observed difference in gliding quality to

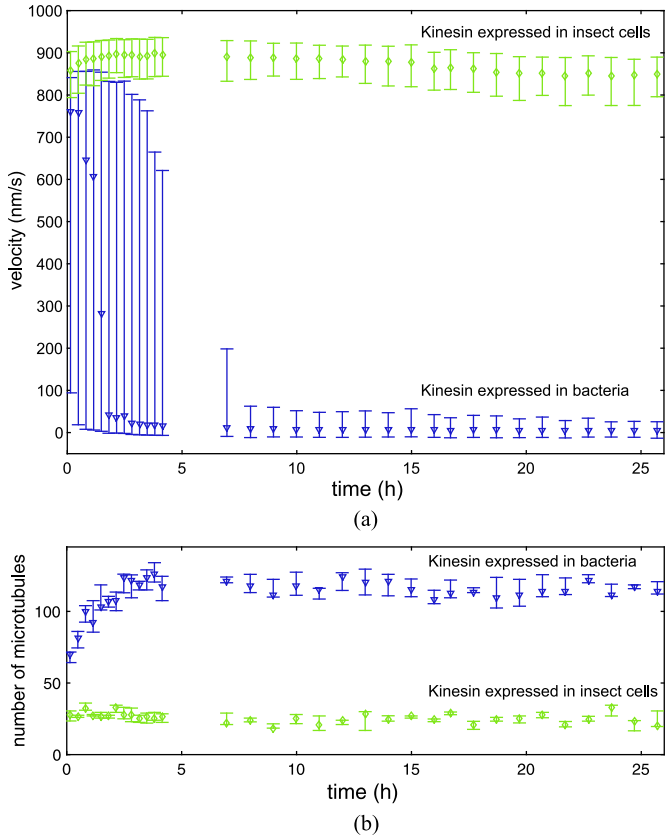

Fig. 3. Long-term stability of the microtubule gliding assay. (a) Microtubule gliding velocities and (b) number of microtubules on kinesin expressed in insect cells (green diamonds) and kinesin expressed in bacteria (blue triangles). (a), (b) The markers and the error bars represent the median and the interquartile range, respectively. In (a) each marker represents 1000–25000 frame-to-frame velocities, in (b) each marker represents the number of microtubules in 3–6 fields of view.

truncated kinesin-1 proteins being the result of premature translation termination in the bacterial expression system [19]. Usually, truncated proteins can be removed during purification by placing the histidine tag used for purification at the C-terminus of the protein (as is the case for our construct used for kinesin expressed in bacteria). This should prevent the truncated proteins (that miss their C-terminus and thus the histidine tag) from being retained in the Ni-NTA column. However, kinesin-1 is a dimer which means that a truncated protein can dimerize with a full-length chain. This potentially generates an "impaired heterodimer," which will still be purified by the affinity column. Such heterodimers may have a shorter coiled-coil stalk than full-length kinesin-1 which likely increases the stiffness of the remaining coiled-coil stalk after binding to a surface. Moreover, a computer model [29] and experiments [30] of microtubule gliding assays with processive kinesin motors have shown, that a low stiffness of the motor proteins is important so that they can work together without hindering each other. Furthermore, impaired dimers could also be generated by misfolding or proteolysis due to chaperones missing in bacteria. This could cause one of the two motor domains to be inactive which has been shown to severely impair the ability of kinesin to propel microtubules in gliding assays [31]. Thus, we postulate that impaired heterodimers are the cause of the aggravated stopping of microtubules propelled by kinesin expressed in bacteria.

The observed stopping of microtubules was probably aggravated by the higher flexural rigidity of double stabilized microtubules [32], which reduces the probability of microtubules bending under force. When the microtubules are straight, all stopped motors more or less equally share the load of the moving motors. Thus in order to detach from the stopped motors, all have to detach simultaneously. In contrast, when the microtubule bends under force, individual stopped motors will experience different local force, which increases the chance that the stopped motors feeling the highest forces detach one after another. See [33] and [5] for experimental demonstrations of such "unzipping" vs. "shearing" mechanisms. The pronounced population of stopped microtubules observed when using double-stabilized microtubules on kinesin expressed in bacteria is likely the reason why double-stabilized microtubules have, so far, not been used more widely for nanotechnological applications. It is certainly the reason why in the past our group has not used these microtubules frequently despite their robustness and shelf-life of several months.

C. Microtubules Propelled by Kinesin Expressed in Insect Cells Do Not Break

In addition to measuring the gliding velocities of microtubules, we also counted the number of microtubules per field-of-view (Fig. 3(b)). For kinesin expressed in bacteria, the number of microtubules rapidly increased during the first 4 h and stayed constant at 117 $\pm$ 8 microtubules/field-of-view for the remainder of the experiment. In contrast, for kinesin expressed in insect cells, the number of microtubules stayed constant at 26 $\pm$ 5 microtubules/field-of-view for the entire experiment.

The initial rapid increase in microtubule number observed for kinesin expressed in bacteria is in agreement with previous reports for taxol stabilized microtubules [10]. However, Brunner *et al.* reported that after 4 h their number of microtubules declined, which is likely because of depolymerization of microtubules stabilized only with taxol. Free microtubules in solution were washed out at the beginning of the experiment. Therefore, the increase in microtubule number can only be explained by breakage. Microtubule breakage likely occurs when the forces during a tug-of-war between moving and stopping motors become higher than the load limit of the microtubule. The absence of breakage of microtubules propelled by kinesin expressed in insect cells confirms that there are much less stopping motors which is in good agreement with the fact that we observed almost no stopped microtubules on kinesin expressed in insect cells. Furthermore, we can rule out photodamage as a reason for microtubule breakage because this would occur on kinesin expressed in insect cells as well as kinesin expressed in bacteria.

The assay time of 26 h is less than the 74 h that a microtubule gliding assay was reported to work under inert atmosphere [11]. However, Kabir *et al.* had to regularly replenish microtubules to compensate for microtubule loss. Because we do not observe loss or breakage of microtubules propelled by kinesin expressed in insect cells even without inert atmosphere, kinesin expressed in insect cells is especially promising for applications such as nanostructured lab-on-a-chip and biocomputation devices where replacing lost microtubules is impossible.

Even longer assay times are likely achievable by combining kinesin expressed in insect cells with an inert atmosphere.

Note Added in Proof: Currently, we have been observing undeteriorated gliding motility in a large-volume chamber sealed with squalane oil (Mansge GmBH) for more than two weeks (ATP was refreshed after 9 days) (personal communication with Bastian Joffroy and Friedrich W. Schwarz).

D. Microtubules Propelled by Kinesin Expressed in Insect Cells are Guided Better in Nanostructures

Robust gliding performance and low loss of microtubules is particularly important for motility in nanostructures, where the total number of microtubules is limited and detachment of microtubules at guiding walls causes additional microtubule loss. To test how kinesin expressed in insect cells affects guiding at walls, we performed microtubule gliding assays in lithographically defined nanostructures where microtubules were gliding on kinesin-1 coated gold surfaces and were guided by 500 nm-high PEG-coated SiO_2 walls (see Fig. 1(c)). A lower flexural rigidity is expected to improve guiding at walls [34], [35]. Therefore, guiding experiments were performed with taxol stabilized microtubules rather than the more rigid double-stabilized microtubules (see methods section). Upon encounter of a wall (Fig. 4(a)), we measured the angle at which the filaments approached the wall and recorded whether they were guided (Fig. 4(a) top row) or detached (Fig. 4(a) bottom row). We then calculated the guiding efficiency (see (1) and (2) in the methods) depending on the approach angle (Fig. 4(b)). For both kinesin-1 expressions, almost all microtubules were guided at approach angles below 30°. For kinesin expressed in bacteria (Fig. 4(b) blue bars), the guiding efficiency dropped to around 50% at angles greater than 45°. In contrast, for kinesin expressed in insect cells (Fig. 4(b) green bars) guiding effieciencies stayed close to 100% up to approach angles of 75°. Even at higher angles (75–90°), the guiding efficiency was still at 83%. The overall average guiding efficiencies were 61 ± 3.8% and 95 ± 1.2% for kinesin expressed in bacteria and kinesin expressed in insect cells, respectively.

The overall guiding efficiency of 95 ± 1.2% observed for kinesin expressed in insect cells is higher than most other guiding efficiencies published for microtubules so far [15], [34], [36], [37] and only surpassed by more complex geometries such as a structure that allowed only small approach angles [38] and channels with undercut walls [39]. In contrast, the guiding efficiency we measured for microtubules propelled by kinesin expressed in bacteria was suboptimal and—particularly at high approach angles—performed less well than previously published results which showed an overall guiding efficiency of 87% and no angle dependency [34]. The reason for this is likely a combination of factors:

a) *Wall height*: The walls used in our chips are only half the height compared to [34].
b) *Wall-angle*: Simulations have shown that wall-angles of less than 90° with respect to the surface can lead to an angle dependency at high approach angles [40]. The results we obtained with kinesin expressed in insect cells agree very well with these simulations, if we assume a wall-angle of 85°. This could indicate that the wall-angle of our structures was not 90° but closer to 85°. However, a lower wall angle cannot explain the difference we observed between kinesin expressed in insect cells and kinesin expressed in bacteria: Our chips were all processed identically and cut from the same wafer. Also, we consistently observed a worse guiding efficiency for kinesin expressed in bacteria compared to kinesin expressed in insect cells on several different chips in several independent experiments.
c) *Wall-bound kinesin-1*: The strong angle dependency we observe for kinesin expressed in bacteria may indicate that in our case the PEGylation of the walls was not perfect and allowed some motors to bind to the wall, potentially decreasing the guiding performance significantly [34], [40]. Thus, the lower guiding efficiency observed with kinesin expressed in bacteria may originate from a higher probability of these motors to bind to the wall than kinesin expressed in insect cells. One reason for the different binding probability could be that—in case of kinesin expressed in bacteria—mainly the impaired heterodimers are binding to the wall.

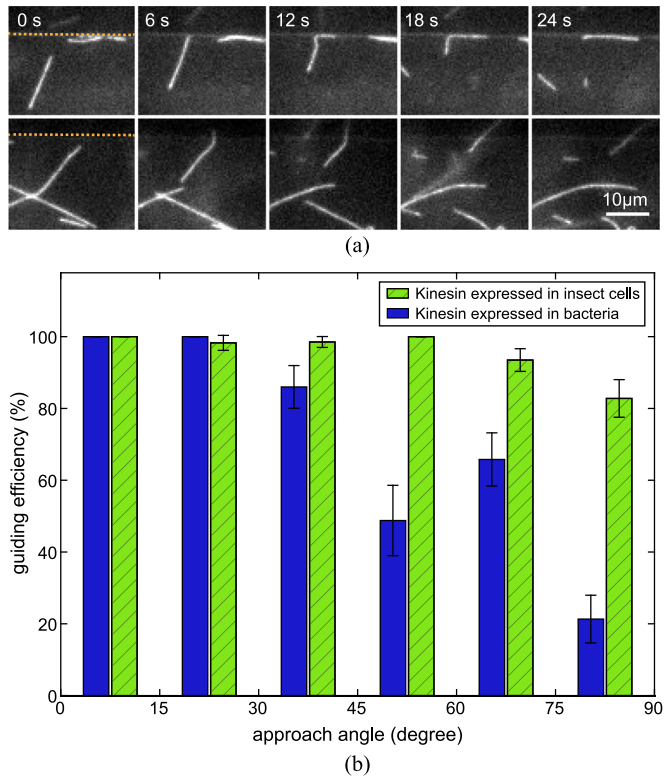

Fig. 4. Guiding efficiencies in lithographically defined nanostructures. (a) Representative fluorescence micrographs of rhodamine labeled microtubules being guided (top row of images) or detaching (bottom row of images) at a PEG-silane coated wall. The position of the wall is indicated by an orange dotted line in the first frame of each row of images. (b) Angle dependence of guiding probabilities of microtubules encountering a wall. Angles were binned in 15° intervals. Microtubules were propelled either by kinesin expressed in insect cells (green bars with diagonal stripes) or kinesin expressed in bacteria (blue, filled bars) Errorbars represent the standard error of the mean of a binomial distribution (see (2) in the Methods section).

IV. Conclusion

We demonstrated that kinesin-1 expressed in insect cells performs far superior to the same protein sequence expressed in

bacteria, when used for *in vitro* gliding motility assays. We observed a constant quality of the gliding motility assay over a period of more than 24 h without having to replenish microtubules or ATP. This expression system also showed improved guiding efficiencies of 95% in lithographically defined nanostructures. Presumably because there are less inactive motors, kinesin expressed in insect cells provides good gliding motility quality even with stiffer, double-stabilized microtubules which eliminates problems with microtubule depolymerization. Because we simply exchanged the expression system to improve the quality of the motor protein, our system is fully compatible with established nanotechnological applications of molecular motors. If necessary, the improved protein expression can also be combined with other methods that prolong the lifetime of motility assays such as immersing the assay in inert gas [11], freeze-drying, or critical point-drying [41], which will most likely result in even further prolonged lifetimes of the assay. Reliability and long-term stability is of practical importance for any nanotechnological device. Therefore, kinesin expressed in insect cells will likely enable the development of bio-nanotechnological devices that perform more complex tasks and are practically useful beyond the proof of principle. Thus we conclude that kinesin-1 expressed in insect cells will enable the use of these motor proteins for more challenging nanotechnological applications than have been demonstrated so far.

Acknowledgment

The authors would like to thank the following services and facilities of the Max Planck Institute of Molecular Cell Biology and Genetics: Protein Expression Facility, Chromatography Facility, Scientific Computing Facility, and Computer Department. In particular the authors would like to thank Aliona Bogdanova for providing the expression vector, Régis Lemaitre for the baculovirus production, Regina Wegner for the insect cell culture, Barbara Borgonovo for help with establishing the protein purification, and Oscar Gonzalez and Peter Steinbach for help with data analysis on a high performance computing cluster. The authors would like to thank the group of Prof. Bartha (TU Dresden), for providing test structures for the microtubule guiding experiments. Furthermore, financial support from the European Union Seventh Framework Programme (grant agreement number 613044, ABACUS), the European Research Council (Starting Grant No. 242933, NanoTrans), the European Social Funds (Grant No. 100111059, MindNano and Grant No. 100107464, ChemIT), and the German Research Foundation (Cluster of Excellence Center for Advancing Electronics Dresden and the Heisenberg Program) is acknowledged.

References

[1] J. Howard, A. J. Hudspeth, and R. D. Vale, "Movement of microtubules by single kinesin molecules," *Nature*, vol. 342, no. 6246, pp. 154–158, Nov. 1989.

[2] H. Hess, "Engineering applications of biomolecular motors," *Annu. Rev. Biomed. Eng.* vol. 13, pp. 429–450, 2011 [Online]. Available: http://www.annualreviews.org/doi/abs/10.1146/annurev-bioeng-071910-124644

[3] T. Korten, A. Månsson, and S. Diez, "Towards the application of cytoskeletal motor proteins in molecular detection and diagnostic devices," *Curr. Opin. Biotechnol.*, vol. 21, no. 4, pp. 477–488, Aug. 2010.

[4] T. Fischer, A. Agarwal, and H. Hess, "A smart dust biosensor powered by kinesin motors," *Nature Nanotechnol.*, vol. 4, no. 3, pp. 162–166, Mar. 2009.

[5] C. Brunner, C. Wahnes, and V. Vogel, "Cargo pick-up from engineered loading stations by kinesin driven molecular shuttles," *Lab on Chip* vol. 7, no. 10, pp. 1263–1271, Sep. 2007 [Online]. Available: http://pubs.rsc.org/en/content/articlelanding/2007/lc/b707301a

[6] D. Steuerwald, S. M. Früh, R. Griss, R. D. Lovchik, and V. Vogel, "Nanoshuttles propelled by motor proteins sequentially assemble molecular cargo in a microfluidic device," *Lab on Chip* vol. 14, no. 19, p. 3729, Jun. 2014 [Online]. Available: http://xlink.rsc.org/?DOI=C4LC00385C

[7] S. Korten, N. Albet-Torres, F. Paderi, L. ten Siethoff, S. Diez, T. Korten, G. te Kronnie, and A. Månsson, "Sample solution constraints on motor-driven diagnostic nanodevices," *Lab on Chip*, vol. 13, no. 5, pp. 866–876, Mar. 2013.

[8] A. T. Lam, C. Curschellas, D. Krovvidi, and H. Hess, "Controlling self-assembly of microtubule spools via kinesin motor density," *Soft Matter* vol. 10, no. 43, pp. 8731–8736, 2014 [Online]. Available: http://pubs.rsc.org/en/content/articlehtml/2014/sm/c4sm01518e

[9] T. Korten and S. Diez, "Setting up roadblocks for kinesin-1: Mechanism for the selective speed control of cargo carrying microtubules," *Lab on Chip*, vol. 8, no. 9, pp. 1441–1447, Sep. 2008.

[10] C. Brunner, K.-H. Ernst, H. Hess, and V. Vogel, "Lifetime of biomolecules in polymer-based hybrid nanodevices," *Nanotechnology* vol. 15, no. 10, p. S540, 2004 [Online]. Available: http://stacks.iop.org/0957-4484/15/i=10/a=008

[11] A. M. R. Kabir, D. Inoue, A. Kakugo, A. Kamei, and J. P. Gong, "Prolongation of the active lifetime of a biomolecular motor for *in vitro* motility assay by using an inert atmosphere," *Langmuir* vol. 27, no. 22, pp. 13 659–13 668, Nov. 2011 [Online]. Available: http://dx.doi.org/10.1021/la202467f

[12] E. L. Dumont, C. Do, and H. Hess, "Molecular wear of microtubules propelled by surface-adhered kinesins," *Nature Nanotechnol.* vol. 10, no. 2, pp. 166–169, 2015 [Online]. Available: http://www.nature.com/articles/nnano.2014.334

[13] D. V. Nicolau, D. V. Nicolau, Jr., G. Solana, K. L. Hanson, L. Filipponi, L. Wang, and A. P. Lee, "Molecular motors-based micro- and nano-biocomputation devices," *Microelectron. Eng.* vol. 83, no. 4–9, pp. 1582–1588, Apr. 2006 [Online]. Available: http://www.sciencedirect.com/science/article/pii/S0167931706001481

[14] D. V. Nicolau, Jr., M. Lard, T. Korten, F. van Delft, M. Persson, E. Bengtsson, A. Månsson, S. Diez, H. Linke, and D. V. Nicolau, "Parallel computation with molecular motor-propelled agents in nanofabricated networks," *Proc. Natl. Acad. Sci.*, DOI:10.1073/pnas.1510825113, to be published.

[15] M. G. L. van den Heuvel, C. T. Butcher, R. M. M. Smeets, S. Diez, and C. Dekker, "High rectifying efficiencies of microtubule motility on kinesin-coated gold nanostructures," *Nano Lett.*, vol. 5, no. 6, pp. 1117–1122, Jun. 2005.

[16] J. Clemmens, H. Hess, R. Doot, C. M. Matzke, G. D. Bachand, and V. Vogel, "Motor-protein "roundabouts": Microtubules moving on kinesin-coated tracks through engineered networks," *Lab on Chip*, vol. 4, no. 2, pp. 83–86, Apr. 2004.

[17] H. Hess, G. D. Bachand, and V. Vogel, "Powering nanodevices with biomolecular motors," *Chemistry*, vol. 10, no. 9, pp. 2110–2116, May 2004.

[18] F. R. Schmidt, "Recombinant expression systems in the pharmaceutical industry," *Appl. Microbiol. Biotechnol.* vol. 65, no. 4, pp. 363–372, Jul. 2004 [Online]. Available: http://link.springer.com/article/10.1007/s00253-004-1656-9

[19] C. Kurland and J. Gallant, "Errors of heterologous protein expression," *Curr. Opin. Biotechnol.* vol. 7, no. 5, pp. 489–493, Oct. 1996 [Online]. Available: http://www.sciencedirect.com/science/article/pii/S0958166996800504

[20] M. Castoldi and A. V. Popov, "Purification of brain tubulin through two cycles of polymerization-depolymerization in a high-molarity buffer," *Protein Express. Purification* vol. 32, no. 1, pp. 83–88, Nov. 2003 [Online]. Available: http://www.sciencedirect.com/science/article/pii/S1046592803002183

[21] D. L. Coy, M. Wagenbach, and J. Howard, "Kinesin takes one 8-nm step for each atp that it hydrolyzes," *J. Biol. Chem.*, vol. 274, no. 6, pp. 3667–3671, 1999.

[22] T. A. Kost, J. P. Condreay, and D. L. Jarvis, "Baculovirus as versatile vectors for protein expression in insect and mammalian cells," *Nature Biotechnol.* vol. 23, no. 5, pp. 567–575, May 2005 [Online]. Available: http://www.nature.com/nbt/journal/v23/n5/abs/nbt1095.html

[23] B. Nitzsche, V. Bormuth, C. Brauer, J. Howard, L. Ionov, J. Kerssemakers, T. Korten, C. Leduc, F. Ruhnow, and S. Diez, "Studying kinesin motors by optical 3d-nanometry in gliding motility assays," *Methods Cell Biol.*, vol. 95, pp. 247–271, 2010.

[24] F. Ruhnow, D. Zwicker, and S. Diez, "Tracking single particles and elongated filaments with nanometer precision," *Biophys. J.* vol. 100, no. 11, pp. 2820–2828, Jun. 2011 [Online]. Available: http://www.ncbi.nlm.nih.gov/pubmed/21641328

[25] E. L. P. Dumont, H. Belmas, and H. Hess, "Observing the mushroom-to-brush transition for kinesin proteins," *Langmuir* vol. 29, no. 49, pp. 15 142–15 145, Dec. 2013 [Online]. Available: http://pubs.acs.org/doi/abs/10.1021/la4030712

[26] R. R. Agayan, R. Tucker, T. Nitta, F. Ruhnow, W. J. Walter, S. Diez, and H. Hess, "Optimization of isopolar microtubule arrays," *Langmuir* vol. 29, no. 7, pp. 2265–2272, Feb. 2013 [Online]. Available: http://dx.doi.org/10.1021/la303792v

[27] V. Schroeder, T. Korten, H. Linke, S. Diez, and I. Maximov, "Dynamic guiding of motor-driven microtubules on electrically heated, smart polymer tracks," *Nano Lett.*, vol. 13, no. 7, pp. 3434–3438, Jul. 2013.

[28] L. Scharrel, R. Ma, R. Schneider, F. Jülicher, and S. Diez, "Multimotor transport in a system of active and inactive kinesin-1 motors," *Biophys. J.* vol. 107, no. 2, pp. 365–372, Jul. 2014 [Online]. Available: http://www.cell.com/article/S0006349514006213/abstract

[29] F. Gibbons, J.-F. Chauwin, M. Despósito, and J. V. José, "A dynamical model of kinesin-microtubule motility assays," *Biophys. J.* vol. 80, no. 6, pp. 2515–2526, Jun. 2001 [Online]. Available: http://www.sciencedirect.com/science/article/pii/S0006349501762236

[30] P. Bieling, I. A. Telley, J. Piehler, and T. Surrey, "Processive kinesins require loose mechanical coupling for efficient collective motility," *EMBO Rep.* vol. 9, no. 11, pp. 1121–1127, Nov. 2008 [Online]. Available: http://embor.embopress.org/cgi/doi/10.1038/embor.2008.169

[31] W. O. Hancock and J. Howard, "Processivity of the motor protein kinesin requires two heads," *J. Cell Biol.* vol. 140, no. 6, pp. 1395–1405, Mar. 1998.

[32] K. Kawaguchi and A. Yamaguchi, "Temperature dependence rigidity of non-taxol stabilized single microtubules," *Biochem. Biophys. Res. Commun.* vol. 402, no. 1, pp. 66–69, Nov. 2010 [Online]. Available: http://www.sciencedirect.com/science/article/pii/S0006291X1001822X

[33] T. L. Fallesen, J. C. Macosko, and G. Holzwarth, "Force-velocity relationship for multiple kinesin motors pulling a magnetic bead," *Eur. Biophys. J.* vol. 40, no. 9, pp. 1071–1079, Jul. 2011 [Online]. Available: http://link.springer.com/article/10.1007/s00249-011-0724-1

[34] J. Clemmens, H. Hess, R. Lipscomb, Y. Hanein, K. F. Bohringer, C. M. Matzke, G. D. Bachand, B. C. Bunker, and V. Vogel, "Mechanisms of microtubule guiding on microfabricated kinesin-coated surfaces: Chemical and topographic surface patterns," *Langmuir* vol. 19, no. 26, pp. 10 967–10 974, 2003.

[35] S. G. Moorjani, L. Jia, T. N. Jackson, and W. O. Hancock, "Lithographically patterned channels spatially segregate kinesin motor activity and effectively guide microtubule movements," *Nano Lett.* vol. 3, no. 5, pp. 633–637, May 2003 [Online]. Available: http://dx.doi.org/10.1021/nl034001b

[36] Y. Hiratsuka, T. Tada, K. Oiwa, T. Kanayama, and T. Q. Uyeda, "Controlling the direction of kinesin-driven microtubule movements along microlithographic tracks.," *Biophys. J.* vol. 81, no. 3, pp. 1555–1561, Sep. 2001 [Online]. Available: http://www.ncbi.nlm.nih.gov/pmc/articles/PMC1301633/

[37] J. Clemmens, H. Hess, J. Howard, and V. Vogel, "Analysis of microtubule guidance in open microfabricated channels coated with the motor protein kinesin," *Langmuir*, vol. 19, no. 5, pp. 1738–1744, 2003.

[38] L.-J. Cheng, M.-T. Kao, E. Meyhöfer, and L. Guo, "Highly efficient guiding of microtubule transport with imprinted CYTOP nanotracks," *Small* vol. 1, no. 4, pp. 409–414, Apr. 2005 [Online]. Available: http://onlinelibrary.wiley.com/doi/10.1002/smll.200400109/abstract

[39] H. Hess, C. M. Matzke, R. K. Doot, J. Clemmens, G. D. Bachand, B. C. Bunker, and V. Vogel, "Molecular shuttles operating undercover: A new photolithographic approach for the fabrication of structured surfaces supporting directed motility," *Nano Lett.* vol. 3, no. 12, pp. 1651–1655, Dec. 2003 [Online]. Available: http://dx.doi.org/10.1021/nl0347435

[40] Y. Ishigure and T. Nitta, "Understanding the guiding of kinesin/microtubule-based microtransporters in microfabricated tracks," *Langmuir* vol. 30, no. 40, pp. 12 089–12 096, Oct. 2014 [Online]. Available: http://dx.doi.org/10.1021/la5021884

[41] M. Uppalapati, Y.-M. Huang, T. N. Jackson, and W. O. Hancock, "Enhancing the stability of kinesin motors for microscale transport applications," *Lab on Chip* vol. 8, no. 2, pp. 358–361, Jan. 2008 [Online]. Available: http://pubs.rsc.org/en/content/articlelanding/2008/lc/b714989a

Authors' photographs and biographies not available at the time of publication.